OPEN ACCESS
IOP PUBLISHING NANOTECHNOLOGY
Nanotechnology **24** (2013) 275604 (10pp) doi:10.1088/0957-4484/24/27/275604

A new bottom-up methodology to produce silicon layers with a closed porosity nanostructure and reduced refractive index

V Godinho[1], J Caballero-Hernández[1], D Jamon[2,3], T C Rojas[1], R Schierholz[1], J García-López[4], F J Ferrer[4] and A Fernández[1]

[1] Instituto de Ciencia de Materiales de Sevilla CSIC-Universidade Sevilla, Avenida Américo Vespucio 49, E-41092 Sevilla, Spain
[2] Université de Lyon, F-42023 Saint Etienne, France
[3] Université Jean Monnet, F-42000 Saint Etienne, LT2C EA 3523, France
[4] Centro Nacional de Aceleradores, Parque Tecnológico Cartuja 93, E-41092 Sevilla, Spain

E-mail: godinho@icmse.csic.es and asuncion@icmse.csic.es (A Fernández)

Received 3 January 2013, in final form 19 March 2013
Published 14 June 2013
Online at stacks.iop.org/Nano/24/275604

Abstract
A new approach is presented to produce amorphous porous silicon coatings (a-pSi) with closed porosity by magnetron sputtering of a silicon target. It is shown how the use of He as the process gas at moderated power (50–150 W RF) promotes the formation of closed nanometric pores during the growth of the silicon films. The use of oblique-angle deposition demonstrates the possibility of aligning and orientating the pores in one direction. The control of the deposition power allows the control of the pore size distribution. The films have been characterized by a variety of techniques, including scanning and transmission electron microscopy, electron energy loss spectroscopy, Rutherford back scattering and x-ray photoelectron spectroscopy, showing the incorporation of He into the films (most probably inside the closed pores) and limited surface oxidation of the silicon coating. The ellipsometry measurements show a significant decrease in the refractive index of porous coatings ($n_{500\,\mathrm{nm}} = 3.75$) in comparison to dense coatings ($n_{500\,\mathrm{nm}} = 4.75$). The capability of the method to prepare coatings with a tailored refractive index is therefore demonstrated. The versatility of the methodology is shown in this paper by preparing intrinsic or doped silicon and also depositing (under DC or RF discharge) a-pSi films on a variety of substrates, including flexible materials, with good chemical and mechanical stability. The fabrication of multilayers of silicon films of controlled refractive index in a simple (one-target chamber) deposition methodology is also presented.

(Some figures may appear in colour only in the online journal)

1. Introduction

Over the past decade research in nanoporous materials has been an expanding field facing a wide range of technological challenges. The continuous advances in silicon based materials in photonic devices, microelectronics and solar energy conversion [1–4], have drawn attention once more to porous silicon [5–7], a material discovered for the first time in 1956 [8]. Being fully compatible with the established microelectronics technology, one of the most attractive features of porous silicon is its customizable refractive index.

Porous silicon has been produced by a variety of approaches, but it is most commonly prepared by electrochemical etching in HF based solutions. Herein, we present for the first time the possibility to produce amorphous porous silicon coatings (a-pSi) with closed porosity by magnetron sputtering. Our approach is a new bottom-up methodology to produce porous silicon coatings with closed and controlled porosity. Recently we reported on the formation of porous silicon oxynitride coatings by magnetron sputtering with a controlled refractive index depending on their deposition conditions [9, 10]. The closed porosity structure with pores filled with molecular nitrogen and aligned in the growth direction allowed the retention of the good mechanical properties characteristic of these coatings. In the present work we show new results following a similar principle to produce porous silicon coatings with closed porosity by magnetron sputtering under controlled deposition conditions.

The application of porous silicon as an antireflective coating (ARC) on silicon solar cells is fully compatible with a closed pore structure [11–14]. Moreover, it is known that chemically etched native porous silicon layers show ageing effects, and thermal oxidation has been considered to ensure their long-term stability, however, increasing the production costs. On the other hand the production of chemical etched porous silicon layers often involves the transfer of these layers to glass substrates [15, 16]; magnetron sputtering allows the direct deposition of large areas of ARC layers on less expensive substrates such as glass. Since no additional heating during deposition is employed, a wide variety of substrates can be used, increasing enormously the possible applications of the a-pSi coatings presented in this paper.

The closed porous structure of these novel magnetron sputtered a-pSi coatings protects the internal pore walls from progressive oxidation. Porous silicon oxidation leads to a lowering of the refractive index, which is critical for its application in photonic devices.

Recently oblique-angle deposition (OAD) of ARC has been presented as a particularly promising method to fabricate nanoporous silicon based films with highly desirable optical properties [17, 18]. In this work oblique-angle magnetron sputtering was also investigated to grow a-pSi coatings with closed pores aligned at a given angle, which can be an interesting way to explore anisotropy in the coatings. The effect of the power supplied to the target on the microstructure and refractive index of porous silicon coatings obtained by oblique-angle deposition is presented.

Another advantage of magnetron sputtering is the ease in producing multilayers of porous and dense material, in this case just by changing the deposition gas. In previous works, Bragg reflectors or microcavities have been produced with alternating low and high refractive index layers prepared by electrochemical methods [19–21]. As a proof of concept, we report in this paper how it is possible to fabricate multilayers of porous and dense silicon just by changing the deposition gas.

The versatility of the fabrication method is finally demonstrated by using intrinsic, p- or n-doped silicon targets. An example of a p-doped amorphous porous silicon coating is presented.

Table 1. Deposition conditions.

Conditions	Setup 1	Setup 2
		
RF power (W)	150	150, 50
Substrate bias (V)	—	—, 100
Target–substrate distance (cm)	10	5
Magnetron angle from vertical (deg)	0	30
Base pressure (Pa)	1×10^{-4}	
Working pressure (Pa)	1.33	
Deposition gases	Ar, He	

2. Experimental details

2.1. Preparation of coatings

In this work we show the possibility of producing a-pSi coatings with closed porosity by magnetron sputtering. Also denser layers were deposited to show the considerable reduction in refractive index achieved by the introduction of porosity.

Table 1 summarizes the deposition conditions. Two setups were used for the deposition of porous coatings. The first (setup 1) uses a cathode placed parallel to the substrate holder at a distance of 10 cm and the second (setup 2), for oblique-angle deposition, has the magnetron head placed at a 30° angle to the normal to the substrate holder and the cathode at a distance of 5 cm from the substrate. In both setups, dense and porous amorphous silicon coatings were deposited from a pure Si target (Kurt J Lesker 99.999% pure) using an RF sputtering source at a power of 150 W. For the OAD, the effects of lower power (50 W) and substrate bias (100 V) were also investigated.

To demonstrate the possibility of also depositing doped silicon coatings with closed porosity, a p-doped Si target from Neyco (boron content of 0.006 at.%, (110) orientation with a resistivity of 0.018 Ω cm) was used. These coatings were deposited using setup 1.

In both setups the base pressure before deposition was 1×10^{-4} Pa. The coatings were deposited at 1.33 Pa using argon to obtain denser coatings and helium to produce coatings with closed porosity. Silicon (100), glass and quartz were used as substrates.

Table 2 summarizes the names used for the prepared samples.

2.2. Characterization of coatings

The thickness and morphology of the samples were studied by scanning electron microscopy (HITACHI S-4800 SEM-FEG).

Table 2. Names used for the samples prepared under different deposition conditions.

Sample	Setup	RF power (W)	Dep. gas	Sub. bias (V)	Deposition rate (nm min^{-1})
a-pSi(0°)	1	150	He	0	7.5
a-Si(0°)	1	150	Ar	0	11.2
a-pSi(30°)(150)	2	150	He	0	15.2
a-pSi(30°)(50)	2	50	He	0	2.6
a-Si(30°)(bias)	2	150	Ar	100	13.0
a-pSi(p-doped)	1	150	He	0	7.5
a-Si(p-doped)	1	150	Ar	0	10.4

The samples were cleaved from coatings grown onto silicon, and were observed without metallization in cross-sectional views at 1–2 kV.

The composition of the coatings was evaluated by x-ray photoelectron spectroscopy. A VG ESCALAB 210 was used, working in the constant analyzer energy mode with a pass-energy of 50 eV. The binding energy reference was taken as the main component of the C 1s peak at 284.6 eV for adventitious carbon. For quantification, the x-ray photoelectron spectroscopy (XPS) spectra were subjected to background subtraction (Shirley background) and sensitivity factors supplied by the instrument manufacturer were used.

The thin film composition was also evaluated by Rutherford backscattering spectrometry (RBS) at the National Center for Accelerators (CNA, Sevilla, Spain) using a 3 MV tandem accelerator. RBS spectra were obtained using two different energies, 1.0 and 2.3 MeV, for the proton beam and a surface barrier detector set at 165°. The lower energy is necessary to separate the Si coming from the substrate and from the film, in order to obtain the sample thickness. The higher energy is required to obtain the He content, because of the energy range where the ^{4}He(p, p$_0$) ^{4}He cross-section is available. To obtain the thickness and composition of the films, both spectra were simulated simultaneously for every sample using the SIMNRA code [22].

The microstructure of the coatings, pore size and distribution, was investigated using a TEM Philips CM200 microscope. Cross-sectional transmission electron microscope (TEM) specimens were prepared in the conventional way by mechanical polishing followed by Ar^+ ion milling to electron transparency. The bonding state of elements in the coating was also evaluated by electron energy loss spectroscopy (EELS) using a PEELS spectrometer from Gatan (mod 766–2 kV) coupled to the TEM. The energy resolution of the microscope/spectrometer system was ∼1.2 eV. All spectra were corrected for dark current and channel to-channel gain variation. A low-loss spectrum was also recorded with each edge in the same illuminated area and using the same experimental conditions. After background subtraction with a standard power law function, the Si-L$_{2,3}$ EELS spectra were deconvoluted for multiple scattering by the Fourier-ratio method. All these treatments were performed within the EL/P program (Gatan).

The optical characterization of the coatings was performed by ellipsometry on samples deposited on quartz substrates. The measurements were executed in a UVISEL spectroscopic ellipsometer from HORIBA Jobin Yvon with an incidence angle of 60° and a wavelength range of 300–2100 nm. The data were analyzed using the Deltapsi2 software developed by HORIBA Jobin Yvon.

3. Results and discussion

3.1. Fundamentals of the methodology

Figure 1(a) is a SEM-FEG cross-sectional view of the structure of a porous silicon coating produced by magnetron sputtering using setup 1 and helium as the deposition gas (sample a-pSi(0°)). As it is possible to observe in this micrograph, and in more detail in figure 1(b), where a TEM cross-sectional view is shown, the coating consists of a dense matrix in which drop-shape closed pores are dispersed. It is possible to appreciate that the closed pores are aligned in the direction of coating growth, with sizes ranging from 10 to 50 nm. For comparison purposes a SEM-FEG cross-section of a dense coating, deposited using argon as the working gas in similar conditions is also presented (figure 1(c) sample a-Si(0°)). This gives evidence of a new kind of porous silicon coating with closed porosity produced by magnetron sputtering. Up to now, the reported PVD or CVD porous silicon coatings were mainly columnar, presenting open porosity [18, 23]. These results demonstrate experimentally that the use of a He plasma in magnetron sputtering deposition equipment is a key factor in controlling the formation of closed porosity. Extensive work is presently being carried out to simulate the microstructure of the growing films by considering the different nature and energy of the species in the Ar and He plasmas. This work will be the subject of a future publication.

EELS studies in TEM can provide the chemical nature of a material. In particular, they are very helpful in understanding the bonding state of elements in materials, as EELS spectra act as 'fingerprints' from the same elemental edge in different compounds [24]. The EELS spectra of both porous (a-pSi(0°)) and dense (a-Si(0°)) TEM cross-sectional samples are presented. Figures 1(d) and (e) show respectively the low-loss and the Si L$_{2,3}$ core-loss edges normalized to the continuum after the edge. The spectra of a silicon monocrystal and an amorphous silicon oxide coating are given as reference. Both silicon coatings, dense and porous, present very similar spectra and are comparable with the reference spectra of the silicon monocrystal, showing the characteristic plasmon resonance at 16.0 eV for bulk Si. The main difference is the broader plasmon peak in the low-loss region for the a-pSi(0°)

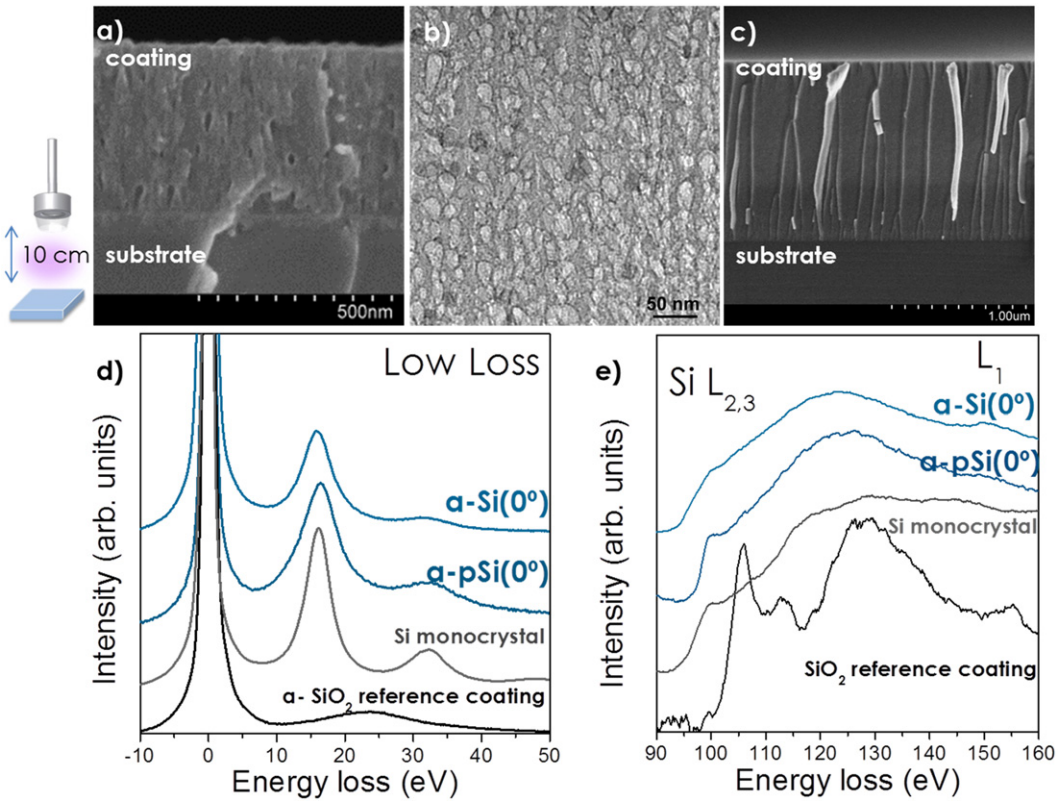

Figure 1. Samples deposited in vertical configuration (setup 1): (a) SEM cross-sectional view of the a-pSi(0°) sample; (b) TEM cross-sectional view of the same sample; (c) SEM cross-section of the a-Si(0°) sample; (d) EELS low-loss and (e) Si core-loss spectra of porous (a-pSi(0°)) and dense (a-Si(0°)) samples compared with reference spectra of an amorphous SiO_2 coating and a pure silicon monocrystal (100).

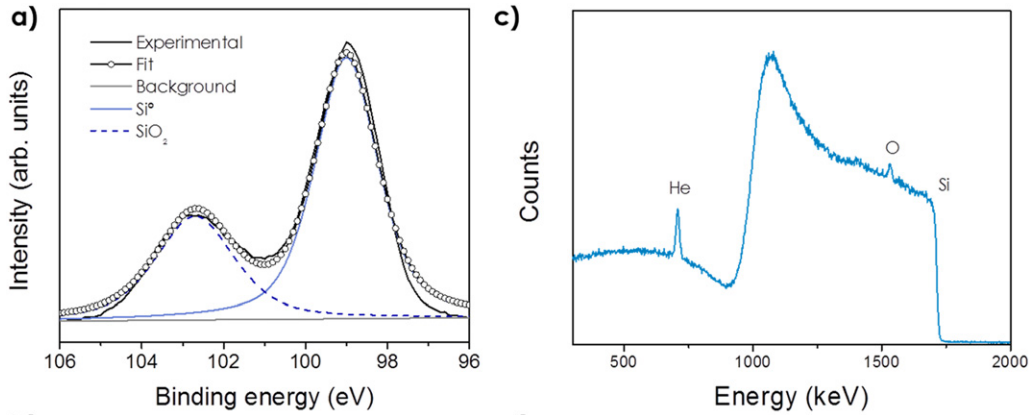

b)

Thickness (nm)	Composition XPS (at%)		
	Si	O	C
450	45	44	10

d)

Thickness 10^{15} atm/cm^2	Composition RBS (at%)		
	Si	O	He
1820	76	10	14

Figure 2. XPS and RBS analysis of the a-pSi(0°) sample: (a) XPS Si2p core level, experimental data and fitted spectra, (b) chemical composition given by XPS, (c) RBS spectrum, (d) thickness and chemical composition given by RBS.

coating, which could be due to the presence of SiO_2 resulting from surface oxidation.

The bonding state of silicon was also evaluated by XPS. Figures 2(a) and (b) show the Si 2p peak and the surface chemical composition of the porous a-pSi(0°) sample. The Si2p peak is composed of a main peak corresponding to elemental Si and a smaller peak corresponding to SiO_2. The ready oxidation of silicon in contact with air is probably the

Table 3. Thickness (given by SEM and RBS) and chemical composition (given by RBS) for selected coatings. Samples named according to table 2.

Sample (setup 2)	RF power (W)	Dep. gas	Thickness (nm) (SEM)	Thickness 10^{15} atm cm^{-2} (RBS)	Composition RBS (at.%) Si	He	Ar
a-pSi(30°)(150)	150	He	450	2 000	66	34	—
a-pSi(30°)(50)	50	He	1000	5 000	66	34	—
a-Si(30°)(bias)	150 (100 V sub. bias)	Ar	4990	18 000	94.0	—	6

main reason for such a high surface oxidation, as indicated by the oxygen content in the table of figure 2(b). The EELS spectra presented are consistent with the hypothesis of surface oxidation of the material.

To evaluate the bulk composition of the porous coating RBS measurements were also performed. Figures 2(c) and (d) show respectively the RBS spectra and a table with the chemical composition obtained. The RBS measurements indicate a very small oxygen content in the coating. This fact confirms the expected high surface oxidation. The RBS measurements also reveal a peak corresponding to the incorporation of He in the coating. The presence of helium seems to point in the same direction as our previous work, where the deposition gas (N_2 in this case) was found inside the pores in silicon oxynitride coatings [10]. The amount of incorporated helium is of the same order of magnitude as previous values obtained by ion implantation experiments in metals [25].

The ability to orient the pores in other directions was also explored in this work; porous silicon coatings deposited with the magnetron axis at 30° to the normal to substrates were produced using setup 2 (table 1). Figures 3(a) and (b) present the porous silicon coatings deposited with helium in glancing incidence at 150 and 50 W respectively. A dense coating deposited with Ar and with a substrate bias was also deposited using the same setup (sample a-Si(30°)(bias), figures 4(a)–(c)).

Figure 3(a1) presents the SEM-FEG cross-sectional view of the a-pSi(30°)(150) sample. It is possible to observe the pores aligned and tilted with respect to the coating growth direction. Figure 3(a2) shows the TEM cross-sectional view of this sample, while the scheme in figure 3(a3) shows the angle (∼17°) that the pores present with respect to the normal of the substrate holder as measured from figure 3(a2). On the magnified TEM images in figures 3(a4) and (a5) it is possible to observe pore sizes ranging from 2 to 42 nm. Selected area electron diffraction (SAED) is also presented as an inset in figure 3(a4), proving that the coating is amorphous.

Decreasing the power supplied to the silicon target at 50 W (figure 3(b)) results in a porous structure with smaller pores, oriented also at ∼17° with respect to the normal to the substrate holder. Figure 3(b1) presents a SEM cross-sectional view of the a-pSi(30°)(50) sample, in this micrograph the pore direction is not easily observed. The TEM cross-sectional view in figure 3(b2) allows one to better observe the pore direction and the scheme in figure 3(b3) shows the angle of the pores. Decreasing the power supplied to the target results in pores ranging from 2 to 23 nm, as measured in the higher magnification images in figures 3(b4) and (b5). Controlling the power supplied to the target allows one to control the pore size while keeping the same pore alignment. Smaller pore sizes can be observed at a lower voltage. The inset in figure 3(b5) shows the amorphous character of the coating.

A very dense coating deposited with a substrate bias is presented in figures 4(a)–(c) for comparison purposes (sample a-Si(30°)(bias)). The TEM and SEM cross-sectional views ((a) and (b) respectively) show a very compact and dense amorphous coating, as proved by the SAED pattern (figure 4(c)).

Figure 5 shows a photograph of the a-pSi(30°)(150) and a-pSi(30°)(50) porous samples deposited directly over glass substrates (1.5 mm thick). The coatings show a red transparent color, characteristic of thin silicon films.

The bulk composition of these coatings was investigated by RBS. Figure 6 and table 3 show the RBS spectra and chemical composition of the coatings deposited by the OAD magnetron sputtering technique (setup 2). The porous silicon coatings deposited at 150 and 50 W are mainly composed of silicon, and present an important He peak (figures 6(a) and (b)). Once more the results indicate the formation of an amorphous matrix with closed pores that may contain the deposition gas inside. For this series of coatings only a small oxygen contamination below the detection limit of the technique under our measurement conditions (5 at.%) was found.

The a-Si(30°)(bias) dense sample, deposited with Ar and under a substrate bias, apart from silicon, shows a small incorporation of Ar, while the amount of oxygen in the coating was below the detection limits for the technique (figure 6 and table 3). Similar results have been published before; the benefits of depositing under an argon atmosphere and the application of a substrate bias to improve the density and prevent oxygen contamination in magnetron sputtered thin films were discussed by Veprek and co-workers [26, 27].

3.2. The optical properties: refractive index

The optical properties of these samples were investigated by ellipsometry. Figure 7 shows the refractive index and extinction coefficient of some representative coatings as a function of the wavelength. Table 4 summarizes the refractive index values at 500 nm. For the a-Si(30°)(bias) dense coating, both the refractive index and coefficient of extinction are high—typical of amorphous silicon [28, 29]. As expected, the introduction of closed porosity leads to an important decrease in the refractive index of the coatings. The porous

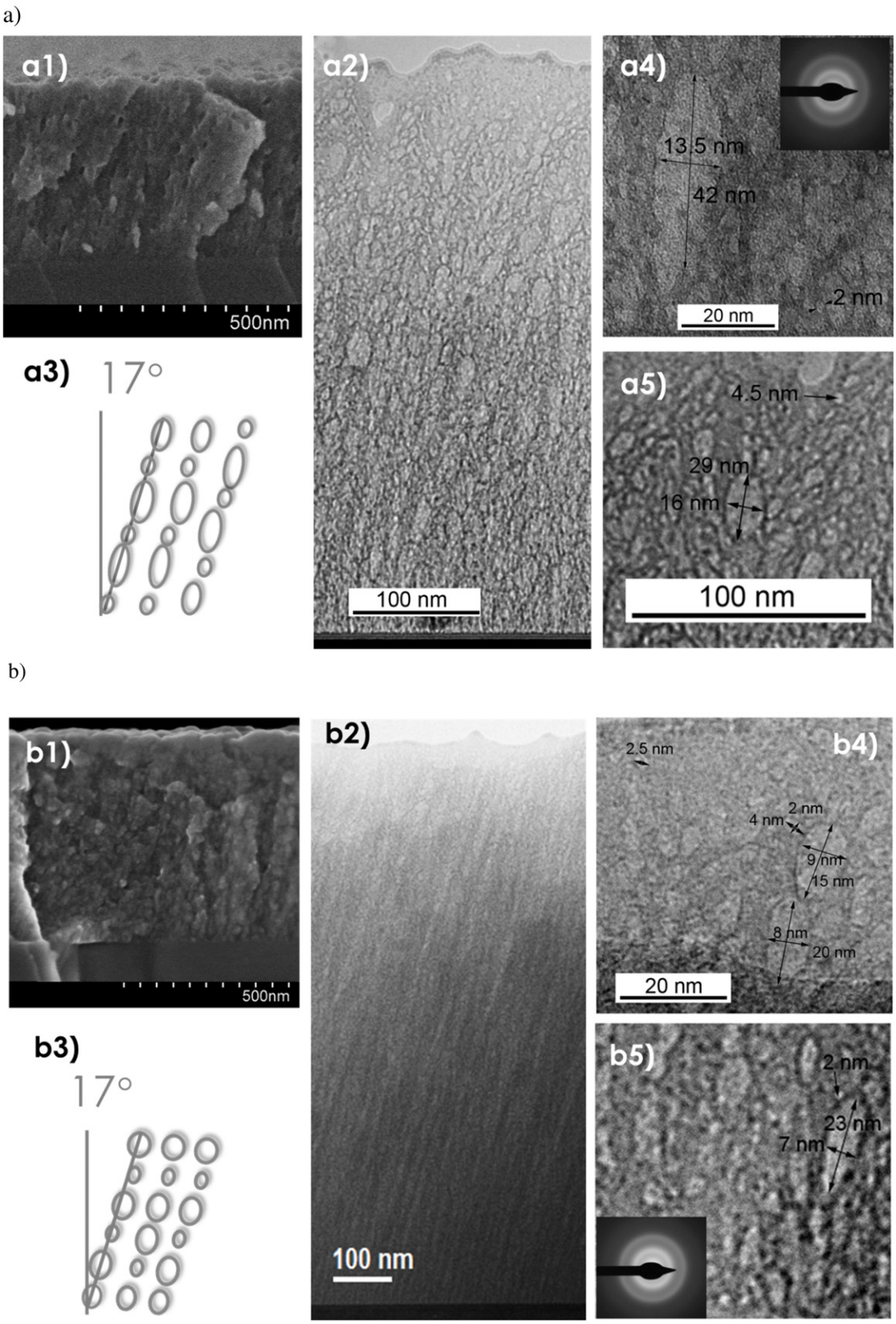

Figure 3. Porous samples deposited under OAD conditions (setup 2). (a) The a-pSi(30°)(150) sample: (a1) SEM cross-sectional view; (a2) TEM cross-sectional view; (a3) scheme of the pore orientation; (a4) detail of TEM micrograph showing the pore size and SAED pattern; (a5) detail of TEM micrograph showing the pore size. (b) The a-pSi(30°)(50) sample: (b1) SEM cross-sectional view; (b2) TEM micrograph showing the sample cross-section; (b3) scheme of the pore orientation; (b4) detail of TEM micrograph showing the pore size; (b5) detail of TEM micrograph showing the pore size and SAED pattern.

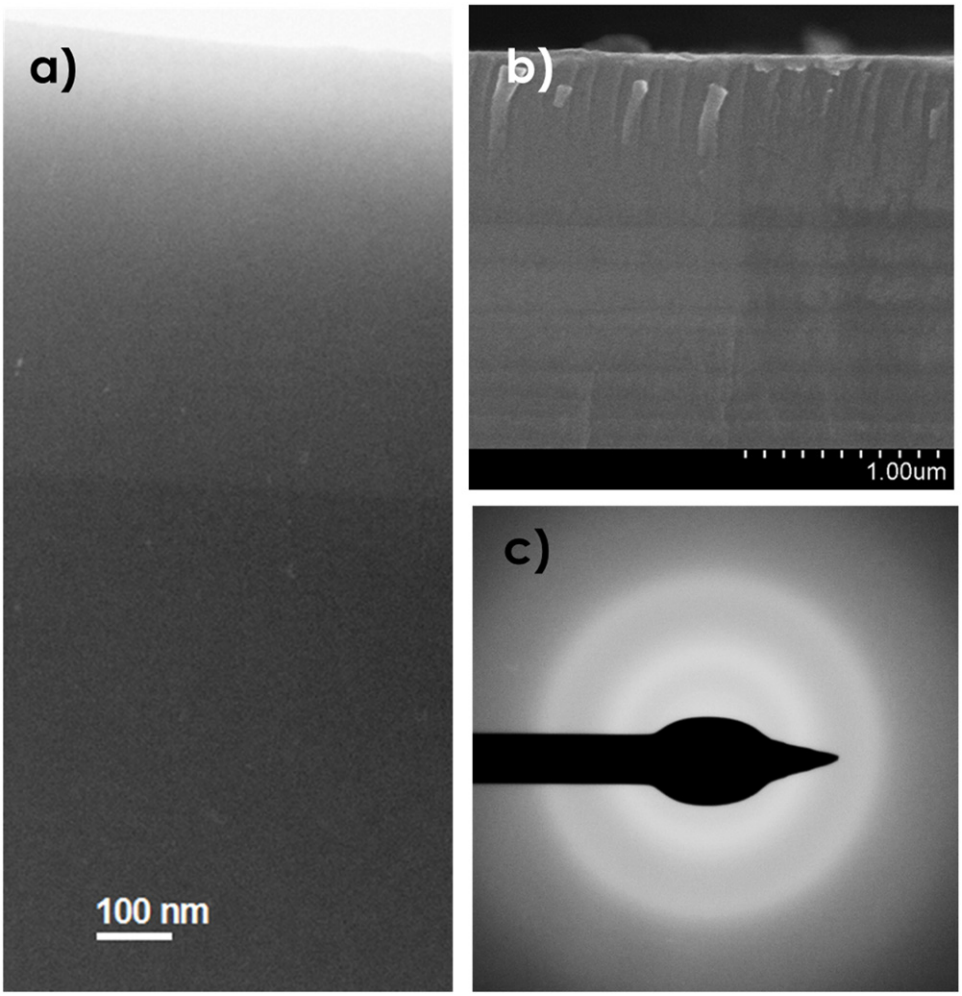

Figure 4. The a-Si(30°)(bias) dense sample: (a) TEM micrograph on the sample cross-section, (b) SEM cross-sectional view, (c) SAED pattern.

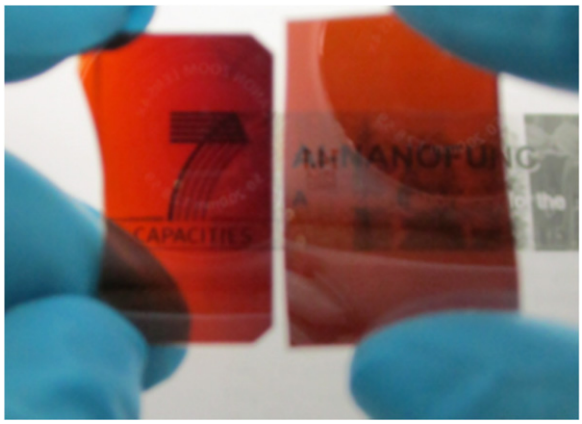

Figure 5. Photograph of the two porous coatings (left a-pSi(30°)(50), right a-pSi(30°)(150)).

a-pSi(30°)(150) and a-pSi(30°)(50) samples, as well as the dense a-Si(30°)(bias) sample, present an oxygen content below 5 at.% according to RBS. The refractive indices for these three samples can be directly compared in table 4. These data demonstrate the capability of the method to control the preparation of porous silicon coatings with a reduced and tailored refractive index. The a-pSi(0°) sample has been selected also because the presence of oxygen (10 at.%) leads to a further reduction of the refractive index, as expected for the formation of silicon oxide phases. This effect is clearly observed both in figure 7 and table 4.

If we take the effective medium approximation, expressing the relative electrical permittivity of a heterogeneous media ($\varepsilon_{r,eff}$), according to the Maxwell–Garnett theory, as a function of the dielectric constants of the continuous ($\varepsilon_{r,c}$) and dispersed phase ($\varepsilon_{r,d}$) it is possible to calculate the volume fraction (ϕ) occupied by the dispersed phase, the pores, according to equation (1):

$$\varepsilon_{r,eff} = \varepsilon_{r,c}\left[1 - \frac{3\phi(\varepsilon_{r,c} - \varepsilon_{r,d})}{2\varepsilon_{r,c} + \varepsilon_{r,d} + f(\varepsilon_{r,c} - \varepsilon_{r,d})}\right]. \quad (1)$$

Considering the dense coating as having the same refractive index as the dense matrix of the porous coatings ($\varepsilon_{r,c}$), and the dielectric constant of the pores ($\varepsilon_{r,d}$) as unity; a porosity fraction ϕ can be estimated for these coatings (see table 4). The values found are consistent with the published refractive index for porous silicon produced by chemical

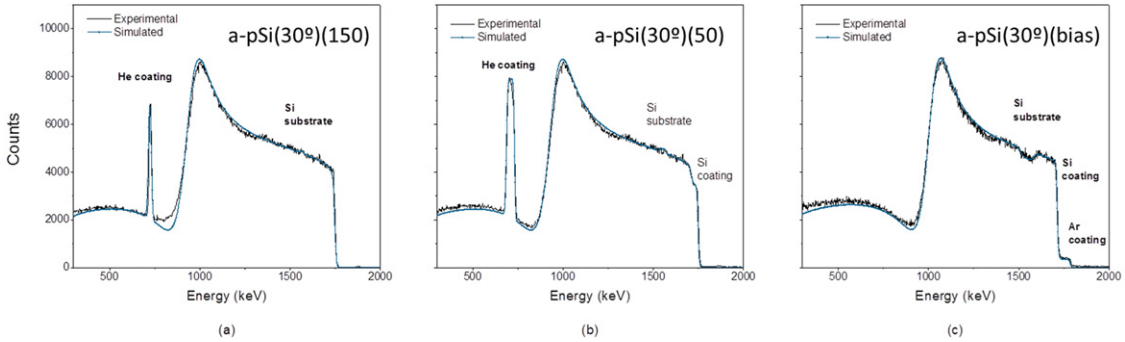

Figure 6. RBS spectra of porous and dense coatings according to the nomenclature described in table 2.

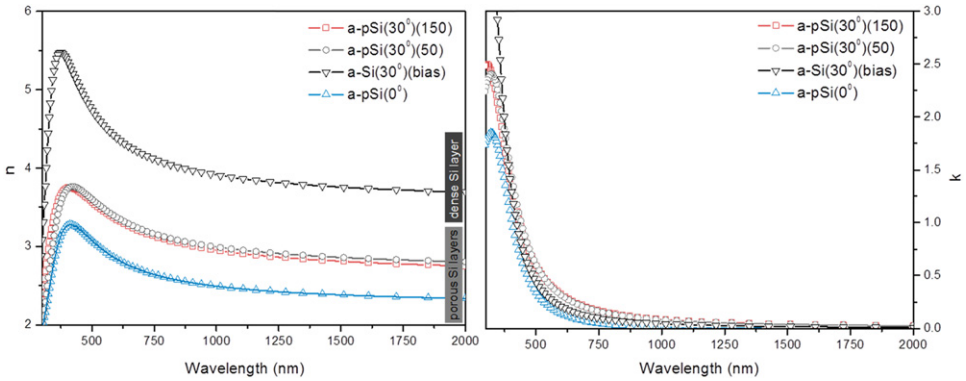

Figure 7. Refractive index (n) and extinction coefficient (k) as a function of the wavelength of porous and dense silicon coatings according to nomenclature described in table 2.

Table 4. Refractive index at 500 nm and porosity fraction calculated from the Maxwell–Garnet equation.

Sample	Power (W)	Dep. gas	Setup	$n_{500\ nm}$ ellipsometry	ϕ[a] (%)
a-pSi(30°)(150)	150	He	2	3.75	30
a-pSi(30°)(50)	50	He	2	3.75	30
a-Si(30°)(bias)	150 (100 V sub. bias)	Ar	2	4.75	—
a-pSi(0°)	150	He	1	3.25	<37[b]

[a] Porosity fraction calculated according to the Maxwell–Garnet equation (1).

[b] The calculated value is an upper limit, as the measured oxidation of the coating (10 at.%, formation of SiO_2) produces an additional decrease of the refractive index as compared to pure porous silicon.

etching with different porosity. Comparing our values with the ones presented by Korotcenkov and Cho [8], porous coatings present porosities between 20 and 40%, which are in good agreement with the values found by the Maxwell–Garnet equation in our coatings. For the a-pSi(0°) sample the calculated porosity fraction (table 4) is an upper limit, as the partial oxidation of the coating (formation of SiO_2) produces a further decrease of the refractive index as compared to pure porous silicon. A careful consideration of the possible formation of the Si–O phases should be considered when comparing the refractive index of this type of coating.

3.3. The versatility of the method

Several experiments have been carried out using He and/or Ar as the process gas, as well as varying different parameters (gas pressure, distance to substrate, power, etc) during magnetron sputtering deposition of silicon coatings. Columnar, dense and closed porous structures have been prepared. Details of all the conditions tested cannot be given in this paper, although some examples of the versatility of the method are presented here.

One advantage of the magnetron sputtered porous silicon films presented in this work is the ease in producing both dense and porous layers in the same setup just by changing the deposition gas. Two examples can be found in figure 8, showing different multilayer structures of alternating denser and closed porous layers. Depending on the deposition conditions, completely dense or columnar layers can alternate with closed porosity layers. This kind of structure with alternating layers with high and low refractive index is the basic principle in the design of Bragg reflectors and optical microcavities [19–21].

So far we have shown results of intrinsic silicon coatings, but it also possible to produce p- or n-doped coatings just by using a doped target. Figure 9 shows, as an example, coatings deposited using a p-doped silicon target. Also in this case it

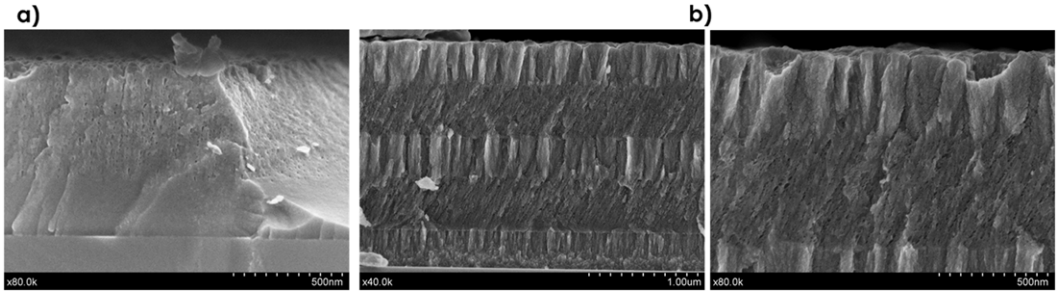

Figure 8. Examples of different possible multilayer structures: (a) Bilayer of dense and porous coatings; (b) multilayer of columnar and porous coatings at two different magnifications.

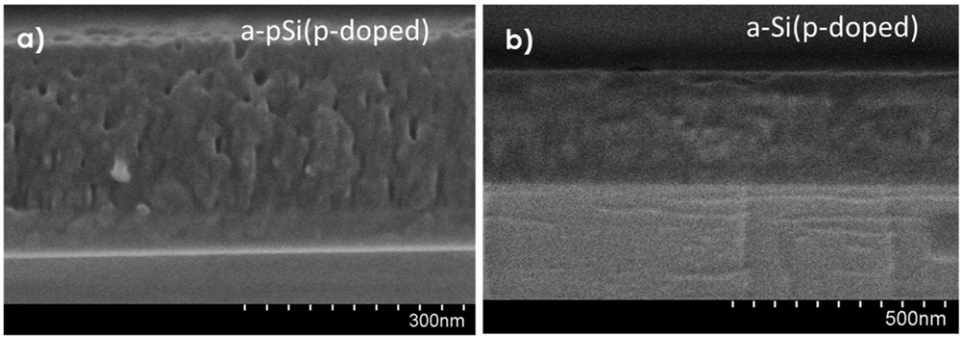

Figure 9. (a) Porous and (b) dense p-doped silicon layers according to the nomenclature in table 2.

is possible to produce porous layers with closed porosity. A dense layer is also presented for comparison; these coatings were deposited using setup 1 and the same conditions as the coatings presented in figure 1. Another advantage of using magnetron sputtering is the possibility to deposit on cheap and or flexible substrates. In figure 4 it is clear that there is the possibility to deposit directly on glass substrates, but the low temperatures achieved also allow the use of polymer substrates. Figure 10 shows the SEM micrographs of a porous layer deposited on a thin and flexible Teflon sheet and on a silicon substrate. These coatings have been grown in the OAD configuration, using DC discharge conditions in this case. The thick layer seems to be very well adhered to the flexible substrate, as one can observe in the photograph presented in figure 10.

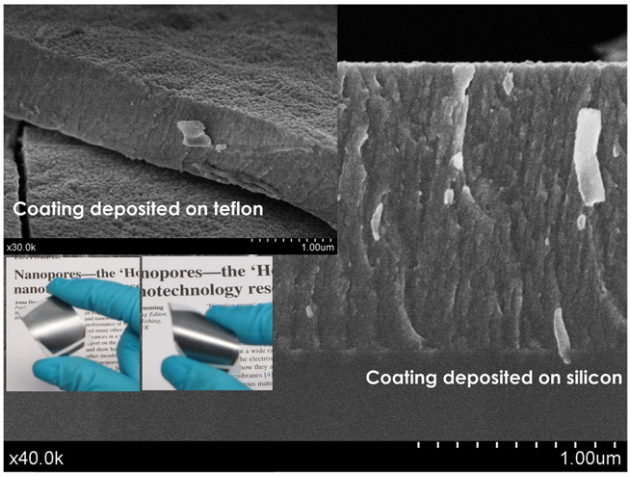

Figure 10. Porous coating deposited under DC discharge conditions on a flexible substrate (Teflon) and the same coating deposited on a silicon substrate.

4. Conclusions

In this work we show a new bottom-up strategy to produce porous silicon coatings with closed porosity, as observed by SEM and TEM micrographs. The formation of closed pores is promoted by the use of He as the process gas during magnetron sputtering deposition at moderate power (50–150 W RF). The EELS and RBS results prove that the coatings are porous silicon and that He is incorporated, most probably inside the pores. The pore size distribution can be changed by changing the power supplied to the target. It is also possible to deposit coatings with different pore orientations by changing the angle of the magnetron.

The introduction of porosity significantly reduces the refractive index of the coatings as compared to dense reference silicon films. The achievement of closed porosity was desired to improve the chemical and mechanical stability as compared to materials previously prepared by etching methodologies with open porosity.

This new methodology allows one to deposit large areas of porous silicon coatings (under DC or RF discharge) on cheap and/or flexible substrates; by alternating the deposition gases also multilayers of porous and dense coatings can be designed according to requirements. The method is presently being successfully extended to other materials.

Future work is under preparation to understand the influence of the complete set of process parameters, both experimentally and theoretically by simulation of the growth processes.

Acknowledgments

The authors are grateful for the financial support from EC (project REGPOT AL-NANOFUNC grant number REGPOTCT-2011-285895-Al-NANOFUNC), CSIC (201160E091, 201060E102) and Spanish Ministry MICINN (CONSOLIDER FUNCOAT).

References

[1] Becker C, Lockau D, Sontheimer T, Schubert-Bischoff P, Rudigier-Voigt E, Bockmeyer M, Schmidt F and Rech B 2012 *Nanotechnology* **23** 135302
[2] Jin H and Liu G L 2012 *Nanotechnology* **23** 125202
[3] Zhang K, Seo J-H, Zhou W and Ma Z 2012 *J. Phys. D: Appl. Phys.* **45** 143001
[4] Spinelli P, Verschuuren M A and Polman A 2012 *Nature Commun.* **3** 692
[5] Dubey R S and Gautam D K 2011 *Optik* **122** 494
[6] Abidi D, Romdhane S, Brunet-Bruneau A and Fave J-L 2009 *Eur. Phys. J. Appl. Phys.* **45** 10601
[7] Ramizy A, Hassan Z, Omar K, Al-Douri Y and Mahdi M A 2011 *Appl. Surf. Sci.* **257** 6112
[8] Korotcenkov G and Cho B K 2010 *Crit. Rev. Solid State Mater. Sci.* **35** 153
[9] Godinho V, de Haro M C J, Garcia-Lopez J, Goossens V, Terryn H, Delplancke-Ogletree M P and Fernandez A 2010 *Appl. Surf. Sci.* **256** 4548
[10] Godinho V, Rojas T C and Fernandez A 2012 *Micropor. Mesopor. Mater.* **149** 142
[11] Fonthal F, Torres I and Rodriguez A 2011 *J. Mater. Sci.—Mater. Electron.* **22** 895
[12] Osorio E, Urteaga R, Acquaroli L N, Garcia-Salgado G, Juarez H and Koropecki R R 2011 *Sol. Energy Mater. Sol. Cells* **95** 3069
[13] Brendel R and Ernst M 2010 *Phys. Status Solidi-Rapid Res. Lett.* **4** 40
[14] Van Hoeymissen J, Depauw V, Kuzma-Filipek I, Van Nieuwenhuysen K, Payo M R, Qiu Y, Gordon I and Poortmans J 2011 *Phys. Status Solidi* A **208** 1433
[15] Solanki C S, Bilyalov R R, Poortmans J, Nijs J and Mertens R 2004 *Sol. Energy Mater. Sol. Cells* **83** 101
[16] Bergmann R B and Werner J H 2002 *Thin Solid Films* **403** 162
[17] Poxson D J, Kuo M-L, Mont F W, Kim Y-S, Yan X, Welser R E, Sood A K, Cho J, Lin S-Y and Schubert E F 2011 *MRS Bull.* **36** 434
[18] Jang S J, Song Y M, Yeo C I, Park C Y and Lee Y T 2011 *Opt. Mater. Express* **1** 451
[19] Birner A, Wehrspohn R B, Gösele U M and Busch K 2001 *Adv. Mater.* **13** 377
[20] Acquaroli L N, Urteaga R and Koropecki R R 2010 *Sensors Actuators* B **149** 189
[21] Chan S and Fauchet P M 2001 *Opt. Mater.* **17** 31
[22] Mayer M 1999 SIMNRA, a simulation program for the analysis of NRA, RBS and ERDA *Proc. 15th Int. Conf. on the Application of Accelerators in Research and Industry* (New York: American Institute of Physics) vol 475, p 541
[23] Patzig C, Khare C, Fuhrmann B and Rauschenbach B 2010 *Phys. Status Solidi* B **247** 1322
[24] Godinho V, Rojas T C, Trasobares S, Ferrer F J, Delplancke-Ogletree M P and Fernandez A 2012 *Microsc. Microanal.* **18** 568
[25] Jager W, Manzke R, Trinkaus H, Crecelius G, Zeller R, Fink J and Bay H L 1982 *J. Nucl. Mater.* **111** 674
[26] Veprek S and Reiprich S 1995 *Thin Solid Films* **268** 64
[27] Veprek S, Veprek-Heijman M G J, Karvankova P and Prochazka J 2005 *Thin Solid Films* **476** 1
[28] Martin P J, Netterfield R P, Sainty W G and McKenzie D R 1983 *Thin Solid Films* **100** 141
[29] Hanyecz I, Budai J, Szilágyi E and Tóth Z 2011 *Thin Solid Films* **519** 2855